

P. Papadopoulos and G. Floudas

Polypeptide Dynamics: Glass "Transition" and "Broken" Helices

i. introduction

Polypeptides are macromolecules composed of amino-acids where hydrogen bonds stabilize certain secondary structures; for example, α -helices are stabilized by intramolecular hydrogen bonds whereas β -sheets by intermolecular hydrogen bonds [1,2]. The α -helical structure, in particular, is thought to give rise to a rigid-rod structure and in this respect poly(γ -benzyl-L-glutamate) (PBLG) has been employed as a model rigid-rod polymer with applications in solution [3], in the melt [4] and on surfaces [5].

The internal dynamics of proteins and other biopolymers at different time and length scales are essential for their function. Here we are mainly concerned with two types of dynamics. The first is associated with the well-known dynamic arrest at a temperature known as the glass temperature (T_g); an essential feature of protein dynamics that can inhibit biological function. Such a dynamic arrest has been observed in a number of different experiments: inelastic neutron scattering [6], Mössbauer spectroscopy [7], infrared spectroscopy [8] and molecular dynamics simulations [9,10]. Although there is consensus about the presence of a dynamic arrest at T_g , its origin is still not well understood. In the first part of this study we provide experimental evidence about the origin of T_g in polypeptides by studying the associated dynamics as a function of molecular weight (M), temperature (T), pressure (P), in solution and as a function of the type of secondary structure. We show that the glass "transition" is an intrinsic property of polypeptides [11].

The second example relates to the relaxation of the α -helical secondary structure. Typical experiments have been performed that confirm the presence of the secondary structure, such as, wide-angle X-ray scattering, NMR and Fourier transform infrared (FTIR) spectroscopy [12]. These experiments are sensitive probes of

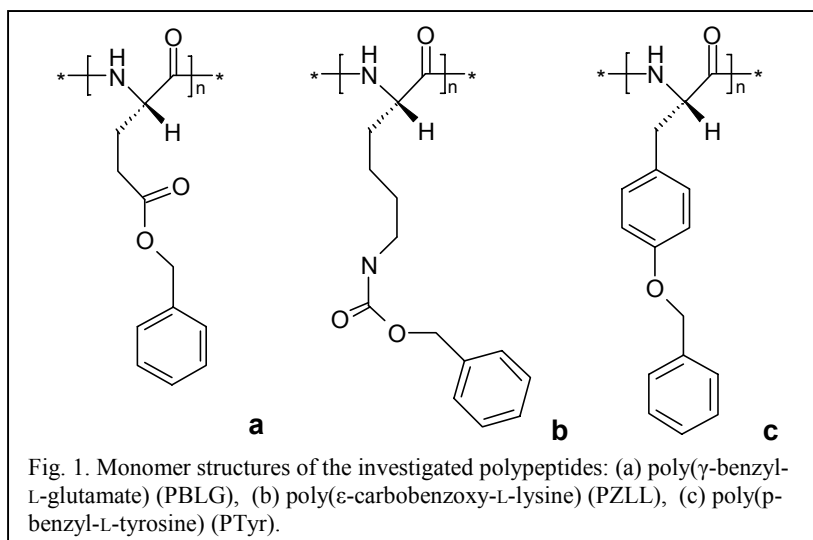


Fig. 1. Monomer structures of the investigated polypeptides: (a) poly(γ -benzyl-L-glutamate) (PBLG), (b) poly(ϵ -carbobenzoxy-L-lysine) (PZLL), (c) poly(p -benzyl-L-tyrosine) (PTyr).

the presence of α -helical segments but the persistence length of such structures cannot be easily obtained. In contrast, dielectric spectroscopy (DS) is extremely sensitive to the coherence of α -helical segments (i.e., the persistence length) therefore DS has been employed as a measure of the "helix perfection" [13]. We show that α -helical polypeptides cannot be considered as ideal rigid rods and that a model of "broken" rods is closer to reality. This has consequences in the self-assembly of polypeptides in block copolymers composed of polypeptide and other synthetic blocks and affects the nanodomain spacing [14]. Furthermore, interfacial mixing in block copolymers may be a way of controlling the appearance of β -sheets in low molecular weight polypeptides [12].

ii. samples

We studied a series of γ -benzyl-L-glutamate polypeptides (PBLG) with varying molecular weights synthesized by Prof. H.-A. Klok (EPFL), one poly(ϵ -carbobenzoxy-L-lysine) (PZLL) and one poly(p -benzyl-L-tyrosine) (PTyr) sample synthesized by Prof. N. Hadjichristidis and H. Iatrou (Univ. of Athens). The monomer structures are shown in Fig. 1. Details on synthesis and characterization procedures can be found elsewhere [11-14].

iii. measurements analysis

The DS measurements were made using a Novocontrol BDS 1260 system. The measurements were

made in the frequency range 10^{-2} – 10^6 Hz and the temperature range 133 – 473 K. We have used two approaches for the data analysis. In the first, the complex permittivity $\epsilon^* = \epsilon' - i\epsilon''$ was used. The dielectric loss curves (ϵ'') were fitted using the empirical Havriliak-Negami equation [15]. The conductivity contribution ($\epsilon''_{\text{cond}} = \sigma_0 / (\omega \epsilon_f)$, where σ_0 is the dc-conductivity and ϵ_f the permittivity of free space) was also taken into account. In some cases the derivative of ϵ' was used ($\epsilon''_{\text{der}} = -\pi/2 \text{ d}\epsilon'/\text{d}(\ln\omega)$) [16], giving rise to a calculated ϵ'' , but without the conductivity contribution. In the second approach we used the electric modulus representation: $M^* = 1/\epsilon^* = M' + iM''$. This representation enables extracting the characteristic times for the ion motion in addition to the molecular dynamics. The relaxation times corresponding to the M'' maximum are close to the ones from ϵ'' and are related through

$$\tau_{M''} = \tau_{\epsilon''} \left(1 + \frac{\Delta\epsilon}{\epsilon_\infty} \right)^{-1/\alpha} \quad (1)$$

in the case of a symmetric ($\gamma_{\text{HN}}=1$) process, where $\Delta\epsilon$ is the dielectric strength of the process under investigation, α is the Havriliak-Negami equation parameter that describes the symmetric broadening of relaxation times distribution and ϵ_∞ is the dielectric permittivity at the limit of high frequencies. The relaxation times discussed below were derived from the M^* representation, whereas for the dielectric strengths the ϵ'' (or ϵ''_{der}) representations were employed.

**iv. results:
dynamics of the liquid-to-glass
“transition” (α -process)**

The origin of the dynamic arrest of protein dynamics at T_g has been a point of controversy. The very broad distribution of relaxation times suggested the freezing of the collective protein dynamics [6] whereas in other cases it was attributed to the reduced solvent mobility [17,18]. A recent investigation [11] have shed some light to this problem, by investigating the liquid-to-glass transition in a series of oligopeptides of γ -benzyl-L-glutamate up to the polymer (PBLG), and in poly(Z-L-lysine) (PZLL) and poly(p-benzyl-L-tyrosine) (PTyr) using dielectric spectroscopy as a function of temperature and pressure. In Fig. 2, the relaxation times associated with the segmental (α -) process of these polypeptides are shown in the usual Arrhenius representation. The relaxation times display a strong non-Arrhenius T-dependence that conforms to the Vogel-Fulcher-Tammann equation

$$\tau_{\max} = \tau_0 \exp \frac{D_T T_0}{T - T_0} \quad (2)$$

where D_T is a dimensionless parameter (with values $D_T=4.9, 7.9$ and 27 for PBLG₄₅, PZLL₁₃₅ and PTyr₇₉, respectively, the numbers give the degree of polymerization) and T_0 is the “ideal” glass temperature ($T_0 = 243, 241$ and 178 K, respectively), located below the calorimetric T_g . The different polypeptides investigated exhibit a

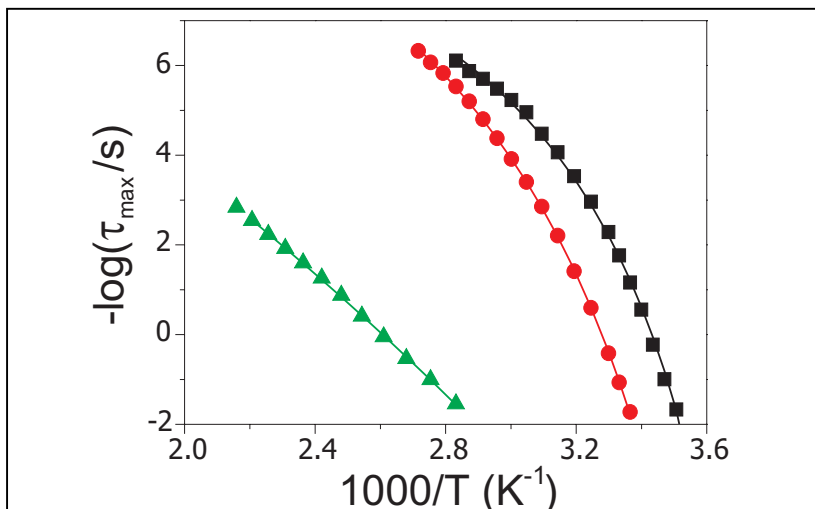


Fig. 2. Arrhenius relaxation map of the segmental processes of PBLG (squares), PZLL (circles) and PTyr (triangles). The lines are fits with the VFT equation. The fragilities of PBLG and PZLL are similar with PZLL being the strongest glass-former but PTyr exhibits a significantly lower fragility.

different $\tau(T)$ dependence; the “fragility” $m(=d \log \tau / d \log (T_g/T)|_{T \rightarrow T_g})$ varies from 69 and 61 for PBLG₄₅ and PZLL₁₃₅ to 24 for PTyr₇₉, suggesting a change from “fragile” to “strong” in going from the purely α -helical peptides to PTyr, which is composed of both α -helices and β -sheets.

This process, in the different polypeptides, is the typical α process found in amorphous polymers and glass-forming liquids associated with the glass-to-liquid relaxation of amorphous segments. This assignment is based on the following: (i) the existence of a step in the specific heat, Δc_p (with magnitudes of 0.49 and 0.37 J/g K for PZLL₁₃₅ and PBLG₄₅,

respectively), (ii) the strong $\tau(T)$ dependence, (iii) the broad and T-dependent distribution of relaxation times (from a Kohlrausch–Williams–Watts stretched exponent of $\beta_{KWW} \sim 0.28$ at T_g to $\beta_{KWW} \sim 0.4$ at $T_g + 30$ K), (iv) the molecular weight dependence of the dynamic T_g , following the Fox–Flory equation: $T_g(x) = 285.9 - 83.7 / \langle x \rangle$ for PBLG, and (v) the pressure dependence. With respect to the latter we have shown that T is the controlling parameter of the dynamics associated with the α -process through the breaking/weakening of hydrogen bonds within the chain and at the chain ends (i.e., at “defects”) [11]. Furthermore, we were able to separate the solvent from the

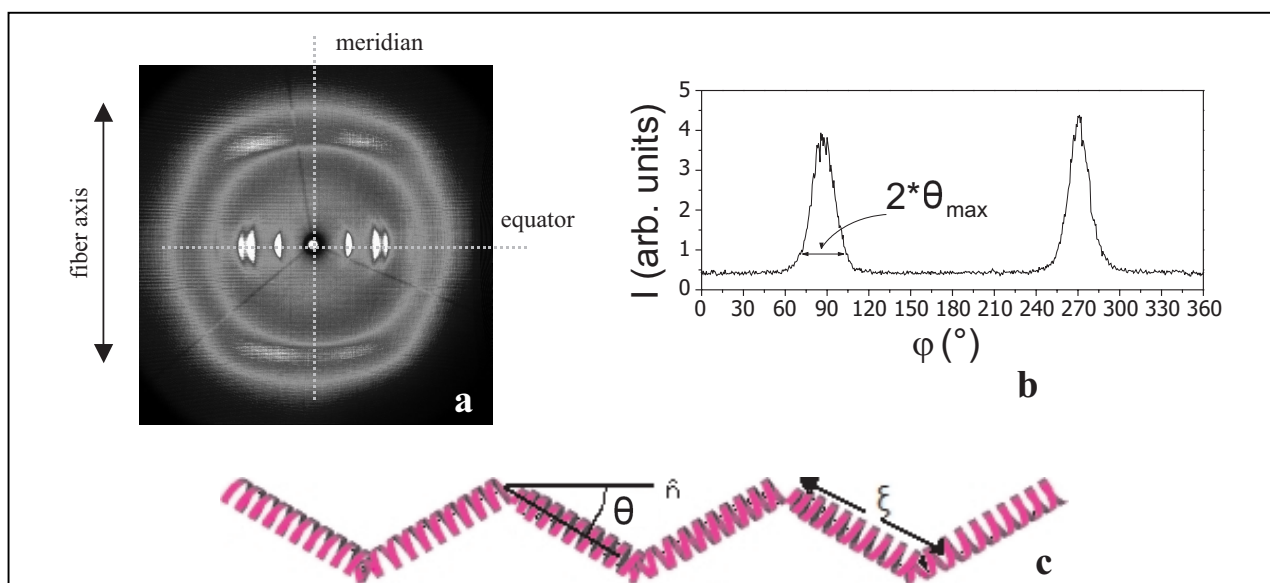


Fig. 3. Model of a “broken” α -helix based on x-ray scattering from oriented PZLL fibers. (a) 2D x-ray pattern from a PZLL fiber extruded at 353 K, annealed and measured at 373 K. The equatorial reflections suggest a hexagonal packing of helices. (b) Azimuthal intensity distribution corresponding to the first equatorial reflection. (c) The “broken” helix is composed of N_p equal parts which can rotate independently around the axis n . The parts are considered “ideal” α -helical. Their length is the persistence length of the secondary structure. The angle θ can be estimated from the width of the peaks in Fig. 3b.

polypeptide α -process in polypeptide solutions [19]. From the above we conclude that the liquid-to-glass “transition” in polypeptides does not relate to the solvent, but is an intrinsic feature of peptide dynamics, irrespective of the type of amino-acid and of the peptide secondary structure. The type of peptide secondary structure, however, plays some role in the exact $\tau(T)$ (and $\tau(P)$) dependencies.

dynamics of the α -helical secondary structure

The existence of an α -helical secondary structure in PBLG and PZLL as well as in other helical-forming polypeptides gives rise to a large dipole moment parallel to the helical axis (typical type-A polymer in Stockmayer's classification) [20]. DS has been employed both in solution and in the melt in studying the dynamics of the secondary structure. The solution studies [3,21,22] were able to identify the large dipole moment per peptide residue (3.4 D) and the exact molecular weight dependence ($\tau \sim M^3$) of the relaxation times. The melt studies [23-27] were mainly concentrated on the glassy phase dynamics and in some cases on the dynamics of the slower process [26,27] attributed to the relaxation of the PBLG helices. In a recent such investigation, α -helices were assumed rigid with their rotation being restricted within a cone rather than being completely free [27]. The essence of this model is also described in the book of Doi and Edwards [28] as the “chopstick” model. In the model, two separate vectors (\vec{u} and \vec{n}) give the polymer and tube directions, respectively, and the two vectors move together like a pair of chopsticks. The external field affects the rapidly moving polymer vector, \vec{u} , which drags the slowly moving tube vector \vec{n} through the coupling potential. This model has similarities with the model proposed by Wand and Pecora [29] for the restricted rotational diffusion of a rod-like molecule within a cone of angle θ_0 . The latter was employed in the study of the molecular dynamics of grafted PBLG [27] and the relaxation strength was shown to scale as

$$\Delta\epsilon_{chopstick} = \Delta\epsilon_{rod} \left(1 - \frac{1}{4} (1 + \cos\theta_0)^2 \right) \quad (3)$$

where $\Delta\epsilon_{rod}$ is the relaxation strength of a freely rotating cone, and θ_0 is the angle of the cone in

Below we outline a model based on “defected” or “broken” helices and provide an estimate of the persistence length ξ , based on the dielectric strength of the slow process.

We start from a freely rotating rigid helix that would give rise to a process with dielectric strength [34]

$$\Delta\epsilon = \frac{N\mu^2}{3\epsilon_0 kT} \quad (4)$$

where N is the number density of helices and μ is the total dipole moment of the helix (which is proportional to the degree of polymerization). In this equation it is assumed that the rotation of each helix is independent from the others (Kirkwood-Fröhlich factor is $g=1$). Furthermore a local field correction factor is not taken into account due to the relatively large size of the helix. Eq. 4 can be rewritten as

$$\Delta\epsilon = \frac{N_A \rho}{3\epsilon_0 kT \langle x \rangle M_m} (\mu_m \langle x \rangle)^2 = \frac{N_A \rho}{3\epsilon_0 kT M_m} \mu_m^2 \langle x \rangle \quad (5)$$

where ρ is the density, $\langle x \rangle$ is the average degree of polymerization, M_m the monomer molecular weight and μ_m the dipole moment per monomer unit. Eq. 5 suggests that for an ideal helix $\Delta\epsilon$ should be directly proportional to $\langle x \rangle$, in contrast to the experiments in bulk PBLG [13]. Notice that the “chopstick” model would give a similar result, i.e., $\Delta\epsilon = (N_A \rho / 3\epsilon_0 kT M_m) \mu_m^2 \sin^2 \theta \langle x \rangle$.

This implies that the helix in the bulk polypeptides cannot be considered as rigid and that it contains “defects”, i.e. broken hydrogen bonds. The “slow” process is therefore attributed to the relaxation of the “broken” helical parts.

In order to quantitatively discuss the origin of defects we propose a model of a “defected” helix, shown in Fig. 3. The helix is assumed to be composed of N_p “ideal” helical parts of equal length ξ (the persistence length) that can rotate on the surface of a cone of angle θ . The rotation of each part is independent from the others, but the axes of all cones are parallel. This is a reasonable assumption, because X-ray measurements from oriented fibers (Fig. 3a) have shown that helices are hexagonally packed. The dipole moment of each part is $\mu_p = 3.4$ Debye*($\xi/0.15$ nm), given that the α -helix length is 0.15 nm/monomer. The total dipole moment is

$$\vec{\mu} = \sum_{i=1}^{N_p} \vec{\mu}_{p_i} = \mu_p \sum_{i=1}^{N_p} (\hat{x} \sin \theta \cos \phi_i + \hat{y} \sin \theta \sin \phi_i + \hat{z} \cos \theta) \quad (6)$$

where ϕ_i is the rotation angle around the axis of the i -th cone. The average value $\langle \vec{\mu} \rangle$ and the average square $\langle \vec{\mu}^2 \rangle$ of the dipole moment are, respectively,

$$\langle \vec{\mu} \rangle = \mu_p \left\langle \sum_{i=1}^{N_p} (\hat{x} \sin \theta \cos \phi_i + \hat{y} \sin \theta \sin \phi_i + \hat{z} \cos \theta) \right\rangle \quad (7)$$

$$= \hat{z} \mu_p N_p \cos \theta$$

$$\langle \vec{\mu}^2 \rangle = \mu_p^2 \left\langle \sum_{i,j=1}^{N_p} (\sin^2 \theta \cos \phi_i \cos \phi_j + \sin^2 \theta \sin \phi_i \sin \phi_j + \cos^2 \theta) \right\rangle \quad (8)$$

$$= \mu_p^2 \left[\sin^2 \theta \left(\sum_{i,j=1}^{N_p} \delta_{ij} \cos^2 \phi_i + \sum_{i,j=1}^{N_p} \delta_{ij} \sin^2 \phi_i \right) + N_p^2 \cos^2 \theta \right]$$

$$= \mu_p^2 (N_p \sin^2 \theta + N_p^2 \cos^2 \theta)$$

The fluctuation dissipation theorem and the linear response theory suggest that μ^2 in Eq. 4 should be replaced by $\langle \vec{\mu}^2 \rangle - \langle \vec{\mu} \rangle^2$. Eq. 4 then yields

$$\Delta\epsilon = \frac{N N_p (\langle \vec{\mu}^2 \rangle - \langle \vec{\mu} \rangle^2)}{3\epsilon_0 kT} \quad (9)$$

$$= \frac{N_A \rho}{3\epsilon_0 kT M_m} (3.4 \text{ Debye})^2 (\xi / 0.15 \text{ nm}) \sin^2 \theta$$

The last equation proposes that $\Delta\epsilon$ is independent of $\langle x \rangle$, in accord with the experimental results [13]. The only parameter that is needed in calculating ξ is the angle θ . The X-ray scattering from oriented fibers (Fig. 3b) can be used to obtain an upper limit, i.e. $\theta_{max} \sim 0.25$ rad. This allows us to calculate a minimum value for ξ , which is plotted in Fig. 4 for a series of PBLG homopolymers. For PZLL this length is ~ 1.4 nm. PTyr forms β -sheets as well as α -helices and therefore the model of Fig. 3 is not valid for the β -sheet part.

which the motion is restricted.

Despite these successes in understanding the dynamics of peptide α -helices there exist theoretical and experimental results in favor of flexibility of PBLG in solution [30-33] and in the bulk [13]. The molecular weight dependence of the PBLG rms radius of gyration in helicogenic solvents [33] indicated some deviations from the expected perfect helix at low and high molecular weights, that could be accounted for by assuming some flexibility and randomness of the chain ends for the lower molecular weights. Similarly, our recent work in undiluted PBLG as a function of molecular weight [13] revealed that both the relaxation times and the associated dielectric strength of the slower process were only weakly dependent on molecular weight, suggesting another origin for the slower process than a mere end-to-end relaxation. A model based on "defected" or "broken" helices is suggested in the inset on the previous page.

The slow process was also

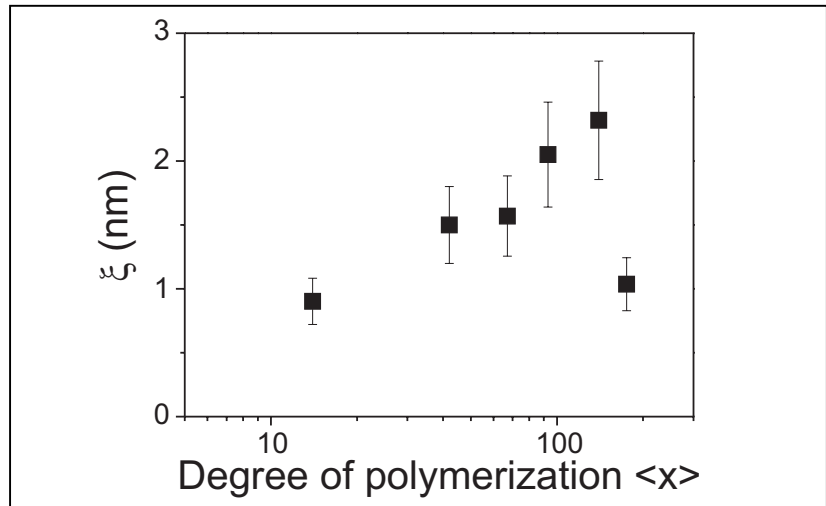


Fig. 4. Persistence length ξ of the α -helical structure for a series of PBLG homopolymers. At low molecular weights it approaches the length of an ideal helix and it is very little affected by the increase of the molecular weight. This persistence length corresponds to ~ 10 monomers.

investigated in a series of PBLG solutions in m-cresol, covering the concentration range from 2% w/w to bulk PBLG [19]. At lower PBLG concentrations the calculated dipole moment reveals nearly rigid helices, but the persistence length decreases

with increasing concentration to about $\sim 20\%$ w/w. Plasticized PBLG, i.e. 80 or 90 % w/w PBLG, exhibits a stronger slow process than pure PBLG and displays a higher persistence length.

ion mobility

In order to investigate the relation between the "slow" process with the ionic conductivity we have created "master curves" of the real and imaginary parts of ϵ^* , M^* and $\sigma^* = \omega \epsilon_0 \epsilon^*$, for PBLG, in Fig. 5, by applying horizontal shift factor a_T to each curve taken at a temperature T , with respect to the curve at the reference temperature. Notice that the crossing of the real and imaginary parts of all quantities occurs at the same frequency, below which dc conduction dominates. Similar results are obtained for the other peptides. The superpositions were made around the M'' maximum corresponding to the conductivity and the same horizontal shift factors were employed for the ϵ^* and σ^* superpositions. Notice that the M'' maximum is always asymmetric, because of the existence of the "slow" process discussed above. This process is more clearly observed in the ϵ''_{der} curves. The position of this peak is in the proximity of the crossing point of σ' and σ'' , which gives the characteristic time of ion motion in the material. The relaxation times of the slow process as well as of the dc conductivity, obtained from the low-frequency plateau in the σ' curves, are plotted together in Fig. 6. Notice the similarity in the $\tau(T)$ and $\sigma_{dc}(T)$ dependencies (both can be described by the VFT equation). Clearly, the ionic conduction and the "slow"

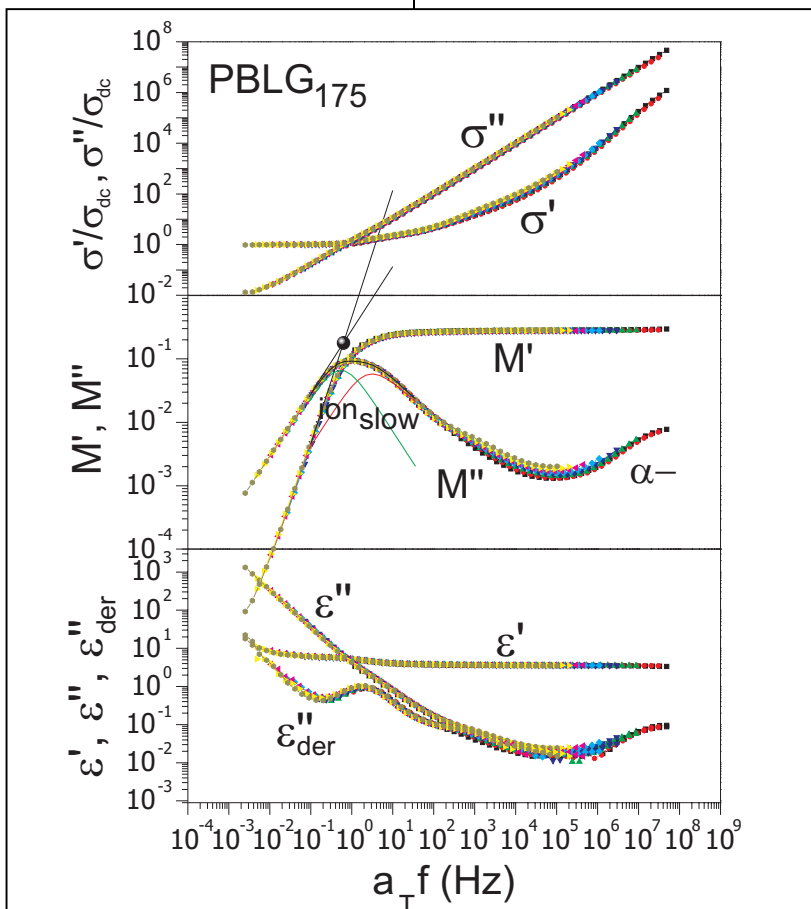


Fig. 5. Simultaneous superpositions of the real and imaginary parts of the conductivity, σ^* , the electric modulus (M^*) and the dielectric permittivity (ϵ^*) for PBLG₁₇₅. The superpositions were made around the M'' maximum. Notice the slow process in ϵ' and ϵ''_{der} in the proximity of M' and M'' crossing, implying that it is coupled to the ionic conductivity. The reference temperature is 413 K.

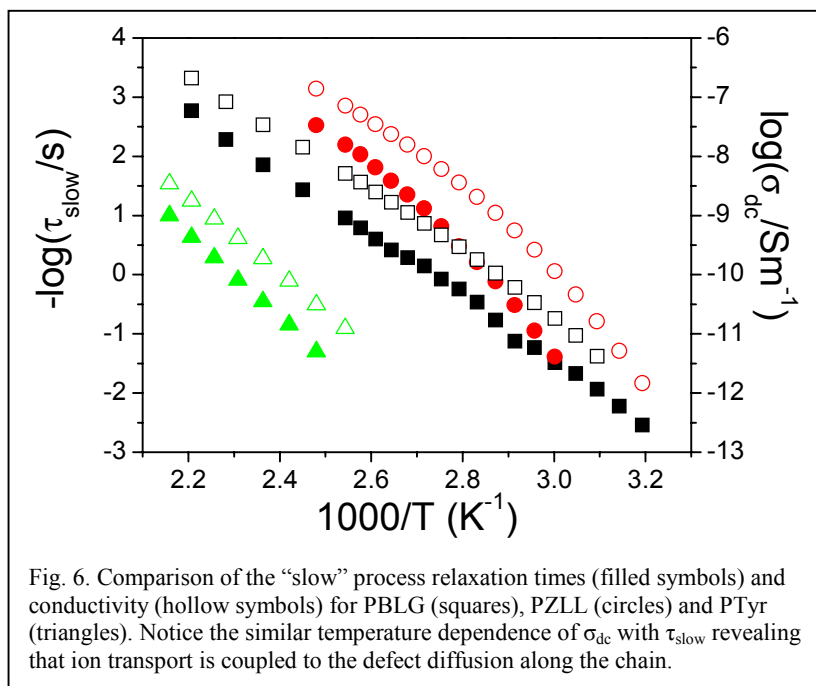


Fig. 6. Comparison of the “slow” process relaxation times (filled symbols) and conductivity (hollow symbols) for PBLG (squares), PZLL (circles) and PTyr (triangles). Notice the similar temperature dependence of σ_{dc} with τ_{slow} revealing that ion transport is coupled to the defect diffusion along the chain.

process are closely related, suggesting that ion transport is coupled to the defect diffusion along the chain. This point deserves further attention.

v. conclusions

Polypeptides are systems rich in dielectrically active relaxation processes, because they have electric dipole moments both on the side chain and along the backbone. Using dielectric spectroscopy as a function of temperature, pressure, polymer molecular weight and the presence of solvent we have shown that the glass “transition” in polypeptides is an intrinsic feature of the peptide dynamics related to the breaking of hydrogen bonds at certain “defected” points along the backbone. Apart from the segmental (α -) process, a slower process exists which reflects the “defect” diffusion along the helix. From the dielectric strength of the slow process we obtain the persistence length of the α -helical structure in the bulk. We show that, contrary to the expectation born out by the static experiments and common belief, helical forming polypeptides are “objects” of low persistence. The ion mobility is nearly coupled to the relaxation of these defects.

acknowledgements

We are indebted to Professors H.-A. Klok (EPFL), N. Hadjichristidis (UoA), H. Iatrou (UoA) for the synthesis and to I. Schnell (MPI-P) for the NMR studies, and to Prof. F. Kremer for making available to us the characteristics of their high molecular weight PBLG sample.

References

[1] Walton, A. G.; Blackwell, J. In *Biopolymers*; Academic Press: New York 1973.
 [2] Block, H. in *Poly(γ -benzyl-L-glutamate) and other glutamic acid containing polymers*; Gordon and Breach Science Publishers: New York, 1983
 [3] Wada, A. *J. Chem. Phys.* **29**, 674 (1958); **30**, 328 (1959); **30**, 329 (1959).
 [4] Yu, S.M.; Soto, C.M.; Tirrell, D.A. *J. Am. Chem. Soc.* **122**, 6552 (2000)
 [5] Jaworek, T.; Neher, D.; Wegner, G.; Wieringa, R.H.; Schouten, A.J. *Science* **279**, 57 (1998)
 [6] Doster, W.; Cusack, S.; Petry, W. *Nature (London)* **337**, 754 (1989)
 [7] Keller, H.; Debrunner, P.G. *Phys. Rev. Lett.* **45**, 68 (1980)
 [8] Iben, I.E.T.; Braunstein, D.; Doster, W. *et al. Phys. Rev. Lett.* **62**, 1916 (1989)
 [9] Smith, J.; Kuczera, K.; Karplus, M. *Proc. Natl. Acad. Sci. USA* **87**, 1601 (1998)
 [10] Norberg, J.; Nilsson, L. *Proc. Natl. Acad. Sci. USA* **93**, 10173 (1996)
 [11] Papadopoulos, P.; Floudas, G.; Schnell, I.; Klok, H.-A.; Aliferis, T.; Iatrou, H.; Hadjichristidis, N. *J. Chem. Phys.* **123** (2005).
 [12] Floudas, G.; Papadopoulos, P.; Klok, H.-A.; Vandermeulen, G.W.M.; Rodriguez-Hernandez, J. *Macromolecules* **36**, 3673 (2003)
 [13] Papadopoulos, P.; Floudas, G.; Klok, H.-A.; Schnell I.; Pakula, T. *Biomacromolecules* **5**, 81-91

(2004).
 [14] Papadopoulos, P.; Floudas, G.; Schnell, I.; Aliferis, T.; Iatrou, H.; Hadjichristidis, N. *Biomacromolecules* **6**, 2352 (2005)
 [15] Havriliak, S.; Negami, S. *Polymer* **8**, 161 (1967)
 [16] Wübbenhorst, M.; van Turnhout, J. *Dielectric Newsletter* **14**, November 2000.
 [17] Vitkup, D.; Melamud, E.; Moul, J.; Sander, C. *Nat. Struct. Biol.* **7**, 34 (2000)
 [18] Rasmussen, B.F.; Stock, A.M.; Ringe, D. and Petsko, G.A. *Nature (London)* **357**, 423 (1992)
 [19] Papadopoulos, P.; Floudas, G. *in preparation*
 [20] Stockmayer, W.H. *Pure Appl. Chem.* **15**, 539 (1967)
 [21] Mori, Y.; Ookubo, N.; Hayakawa, R.; Wada, Y. *J. Polym. Sci., Polym. Phys. Ed.* **20**, 211 (1982)
 [22] Moscicki, K.; Williams, G. J. *Polym. Sci., Poly. Phys. Ed.* **21**, 197 (1983)
 [23] Romero Colomer, F.J.; Gómez Ribelles, J.L. *Polymer* **30**, 849 (1989)
 [24] Romero Colomer, F.J.; Gómez Ribelles, J.L.; Barrales-Rienda, J.M. *Macromolecules* **27**, 5004 (1994)
 [25] Watanabe, J.; Uematsu, I. *Polymer* **25**, 1711 (1984)
 [26] Schmidt, A.; Lehmann, S.; Georgelin, M.; Katana, G.; Mathauer, K.; Kremer, F.; Schmidt-Rohr, K.; Boeffel, C.; Wegner, G.; Knoll, W. *Macromolecules* **28**, 5487 (1995)
 [27] Hartmann, L.; Kratzmüller, T.; Braun, H.-G.; Kremer, F. *Macromol. Rapid Commun.* **21**, 814–819 (2000).
 [28] Doi, M.; Edwards, S.F. *The Theory of Polymer Dynamics Oxford Univ. Press Inc., New York* (1986).
 [29] Wang, C.; Pecora, R. J. *Chem. Phys.* **72**, 5333 (1980)
 [30] Zimm, B.H.; Bragg, J.K. *J. Chem. Phys.* **31**, 526 (1959)
 [31] Flory, P.J. *Macromolecules* **11**, 1126 (1978)
 [32] Flory, P.J.; Frost R.S. *Macromolecules* **11**, 1134 (1978)
 [33] Muroga, Y.; Nagasawa, M. *Biopolymers* **45**, 281–288 (1998).
 [34] *Broadband Dielectric Spectroscopy*, Kremer, F.; Schönhals, A. (Eds), *Springer: New York* (2003)
 Prof. P. Papadopoulos and Prof. G. Floudas, University of Ioannina, Dept. of Physics, P.O. Box 1186, 451 10 Ioannina and Foundation for Research and Technology-Hellas (FORTH), Biomedical Research Institute (BRI)

Yoshihito Hayashi, Anna Gutina, and Yuri Feldman

Low Frequency Liquid Sample Holder: Three Electrode Type

introduction

The study of the complex dielectric properties of liquid samples in wide frequency and temperature ranges is not an easy task. Usually a plate capacitance, consisting of two electrodes and spacers, is used for low frequency measurements of liquids. However, with such conventional sample cells one can be faced with a number of problems. For example leakage, thermal expansion of the liquid sample (and the uncontrollable pressure changes that result), unacceptable reproducibility (especially in the amplitude of permittivity) and difficulties of proper calibration of the sample cell (including an estimation of the fringing field effects). Moreover the measurements of liquids with low viscosity are almost impossible to conduct with such a sample holder. In spite of the scientific community's demand for a reliable liquid sample cell for dielectric measurements, there is still lack of such a critical element in most dielectric laboratories. Here we introduce a specially designed cylindrical sample holder that prevents most of the above mentioned problems. The cell is available from Novocontrol as "BDS 1307 cylindrical sample cell".

configuration of the new sample holder

Figure 1 shows photographs and a schematic drawing of the sample holder for a frequency range lower than 3 MHz. The principal behind the design is to allow the liquid to freely expand according to the temperature condition, thus maintaining the more usual thermodynamic demand of constant pressure rather than constant volume. However, the inclusion of a guard electrode concentrates the electric probing field into a constant volume allowing a fixed geometric capacitance of the sample cell.

The inner electrode looks is a cap that covers a central column of Teflon. This column reduces any parasite capacitance between the inner electrode and the external metal container. The outer- and the guard- electrodes are ring shaped and are isolated one from the other by a thin Teflon ring. Through a connection pin, the guard electrode is grounded using the connecting wire

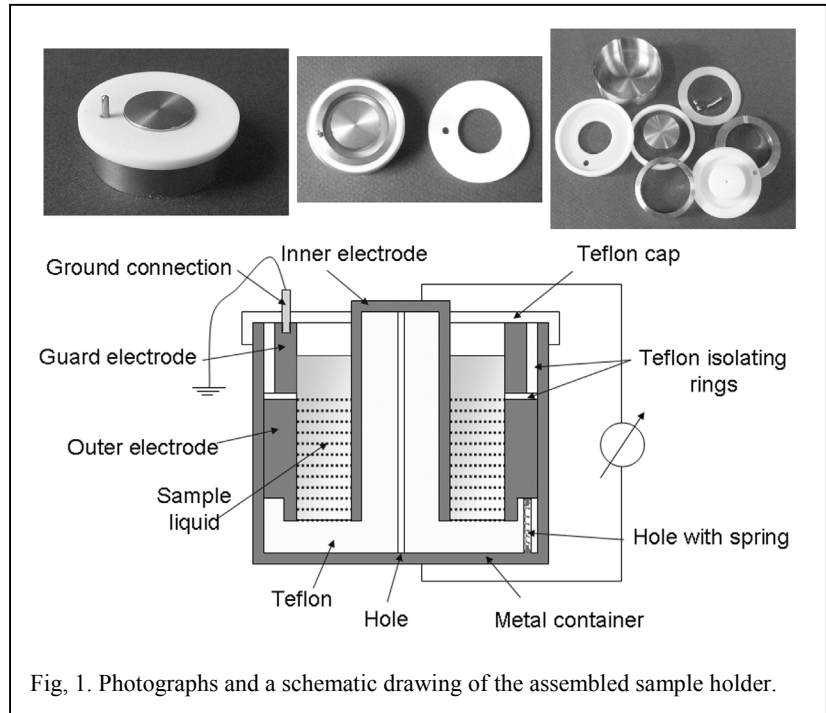


Fig. 1. Photographs and a schematic drawing of the assembled sample holder.

to the grounded parts of the original Novocontrol sample cell. A liquid sample should be fill the sample holder approximately up to the middle level of the guard electrode. The effective measuring region is marked by broken lines in the schematic drawing in Figure 1. The liquid sample cell can be mounted between the standard electrode plates of the Novocontrol sampling head.

advantages of the new sample holder

The main advantages of this sample cell are:

- Good reproducibility: In general for dielectric measurements of liquids, the mounting of the sample and the setting the electrodes without air bubbles is critical. In conventional sample cells with plate electrodes, however, it is difficult especially for highly viscose samples. Moreover it is almost impossible to check after closing the sample cell that it is indeed free of air bubbles. The presence of bubbles can reduce measured capacitance values and therefore be source of error in the amplitude of the complex permittivity. Even if the mounting of the sample and closing of a sample cell are successful, air bubbles can appear during BDS measurements, especially at higher temperatures if degassing of the sample was not completed beforehand. In the case of conventional sample cells, it is very difficult to check after the measurements if air bubbles have

appeared or not. In contrast, it is much easier on the new sample holder. After BDS measurements, one can take out Teflon cap in Figure 1 without disturbing the sample, and can see by eye (or with a magnifying glass) the presence of any air bubbles.

- Constant pressure and no liquid leakage

Because it is not necessary to fill the sample cell up to the top level of the guard electrode, liquid leakage as a result of thermal expansion is avoided even close to the boiling point. There is enough space for thermal expansion of the liquid so that the pressure of the liquid sample is not affect.

- Minimum fringing field effects

The effects of the fringing field are minimized by the guard electrode as shown in Figure 1. Moreover, the remaining small effects can be calibrated out by using a set of standard sample measurements when first using of the sample cell.

calibration procedure

The geometric capacitance of the cylindrical liquid sample cell C_{0_geom} can be calculated using the formula:

$$C_{0_geom} = \frac{2\pi\epsilon_0 L}{\ln \frac{b}{a}}, \quad (1)$$

where $\epsilon_0 = 8.85 \cdot 10^{-12}$ F/m is the dielectric permittivity of vacuum, L is the height of the outer electrode, b and a are diameters of the outer and inner electrodes, respectively. In

order to improve the accuracy, it is recommended to calibrate the sample holder by using standard samples (water, acetone, methanol, ethanol, air, etc.). In fact, C_{0_geom} can be smaller than the real value of the empty capacitance (C_{0_real}) and there is an additional parasitic capacitance C_{add} , which can be subtracted from the measured capacity C_m by the Novocontrol WinDETA program. The C_{add} capacitance is in parallel with the sample capacity and remains constant for any measurements, thereby contributing to only real part of the complex permittivity. Therefore, the measured capacitance C_m can be described with a measurement of a standard sample as:

$$C_m = \epsilon_m C_{0_geom} = \epsilon_{real} C_{0_real} + C_{add} \quad (2)$$

where ϵ_m and ϵ_{real} are the measured static dielectric permittivity and the real permittivity (known value) of the standard sample at measured temperature. By using two standard samples (for example water and air), one can obtain two unknown values of C_{0_real} and C_{add} . The obtained value of C_{add} should be placed under the ‘‘Cell Stray + Spacer Capacity [pF]’’ description in the Sample Specification window of the WinDETA program. Furthermore, C_{0_real} should be used instead of C_{0_geom} for sample measurements.

typical example:
glycerol-water mixtures

Figures 2 and 3 show typical dielectric spectra of glycerol-water mixtures as examples of higher- (90 mol % glycerol, Figure 2) and lower- (30 mol % glycerol, Figure 3) viscous liquids [1, 2]. The main relaxation process and dc conductivity behaviour is observed. In the case of 90 mol % glycerol, high frequency ‘‘excess wing’’ is also found [1].

References

- [1] A. Puzenko, Y. Hayashi, Ya. E. Ryabov, I. Balin, Yu. Feldman, U. Kaatze and R. Behrends, *J. Phys. Chem. B* **109**, 6031-6035 (2005).
- [2] Y. Hayashi, A. Puzenko, I. Balin, Ya. E. Ryabov and Yu. Feldman, *J. Phys. Chem. B* **109**, 9174-9177 (2005).

Dr. Yoshihito Hayashi, Dr. Anna Gutina, and Prof. Yuri Feldman
Department of Applied Physics, The Hebrew University of Jerusalem, Givat Ram, 91904, Jerusalem, Israel

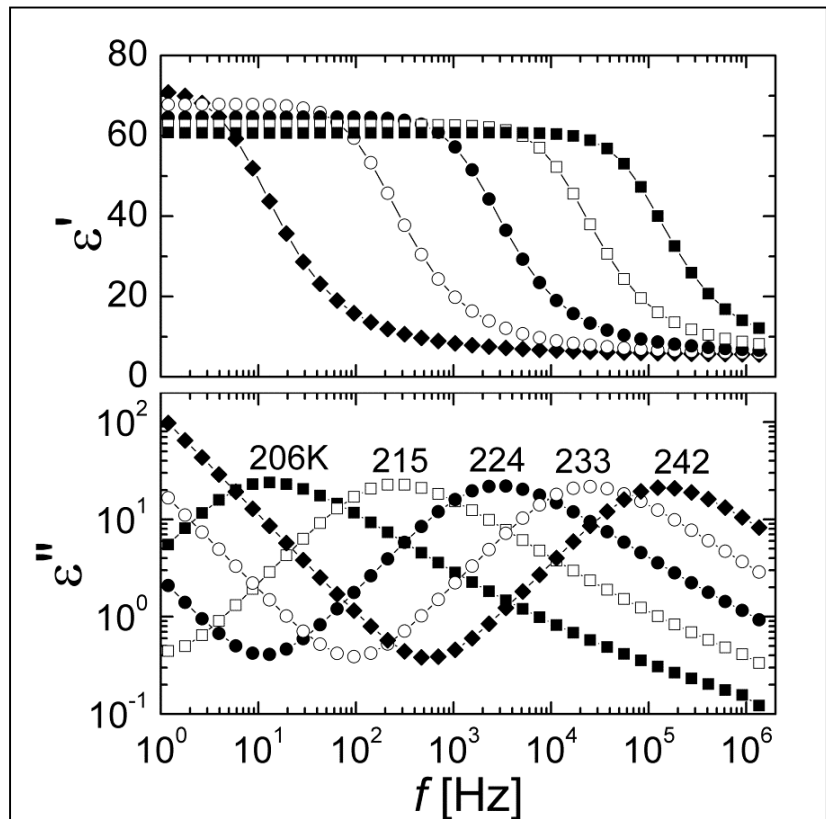


Fig. 2. Dielectric spectra of higher viscous liquid (90 mol.% of glycerol-water mixture, 510 mPa_s at 298 K) at various temperatures.

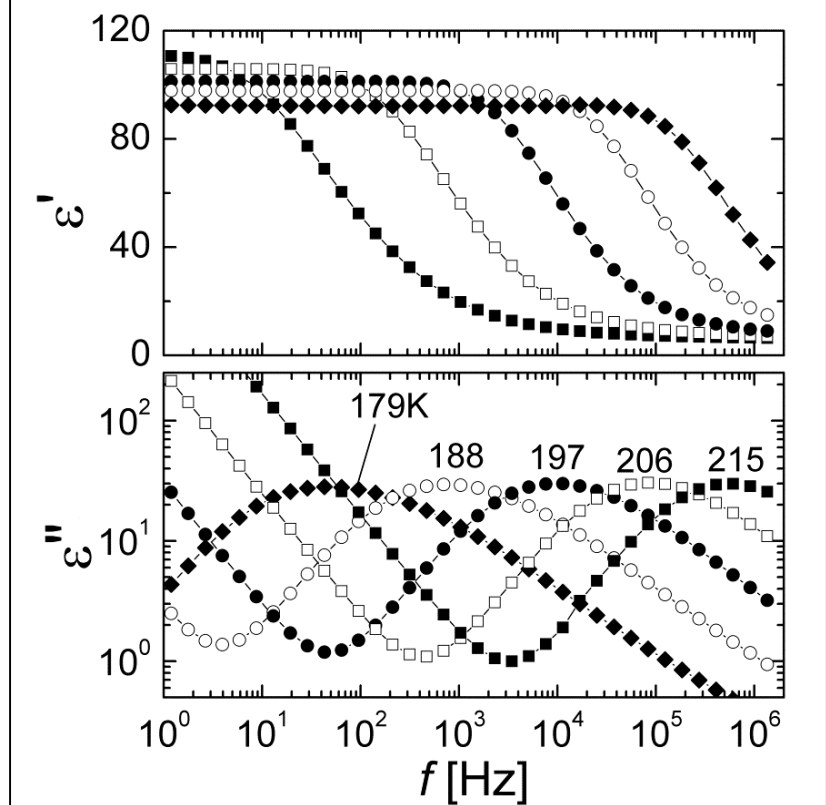


Fig. 3. Dielectric spectra of lower viscous liquid (30 mol.% of glycerol-water mixture, 17.1 mPa_s at 298 K) at various temperatures.

A. Serghei, F. Kremer

Impact of the Experimental Conditions on the Dynamics of Thin Polymer Films

During the last decade the dynamics of glass forming materials in geometrical confinement has attracted a large experimental and theoretical interest [1-13]. One of the most intensively investigated systems represent thin polymer films [5-13], for which deviations of the dynamic glass transition from its bulk behaviour – denoted as confinement effects or finite size effects – have been often reported. Due to highly controversial experimental results [14,15], confinement-effects are at present intensively discussed in the scientific community.

A factor to which not enough attention has been paid in numerous investigations represents the impact of the experimental environment on the properties of thin polymer films. Due to a strongly enhanced surface-to-volume ratio which increases the area of exposure to the ambient environment, these systems are extremely sensitive to the presence of water-vapour and oxygen. Thus, non-appropriate experimental condi-

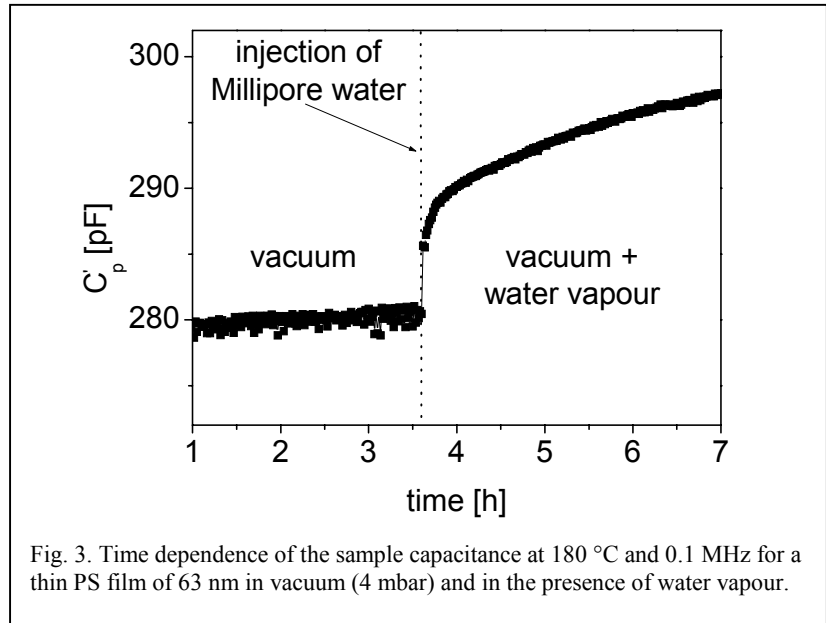


Fig. 3. Time dependence of the sample capacitance at 180 °C and 0.1 MHz for a thin PS film of 63 nm in vacuum (4 mbar) and in the presence of water vapour.

tions can lead – through plasticizer and chain-scission effects – to undesirable changes in the molecular dynamics of the polymers under study. In the present work we show that thin polystyrene films exhibit an enhanced mobility in ambient air, while in an inert atmosphere (pure nitrogen) they turn out to be stable in terms of their dielectric response.

Thin polystyrene films (Mw=700,000 g/mol, polydispersity < 1.05) are prepared by spin-coating from a toluene solution on an

aluminium electrode. After annealing (12 hours at 150 °C in an oil-free high vacuum, 10⁻⁶ mbar) a second aluminium counter-electrode is thermally evaporated on top of the polymer films. A detailed description of the preparation procedure can be found in [16]. The thickness is determined using the capacitive method [11], under the assumption that the real part of the complex permittivity function does not show a thickness dependence in the limit of high-frequencies.

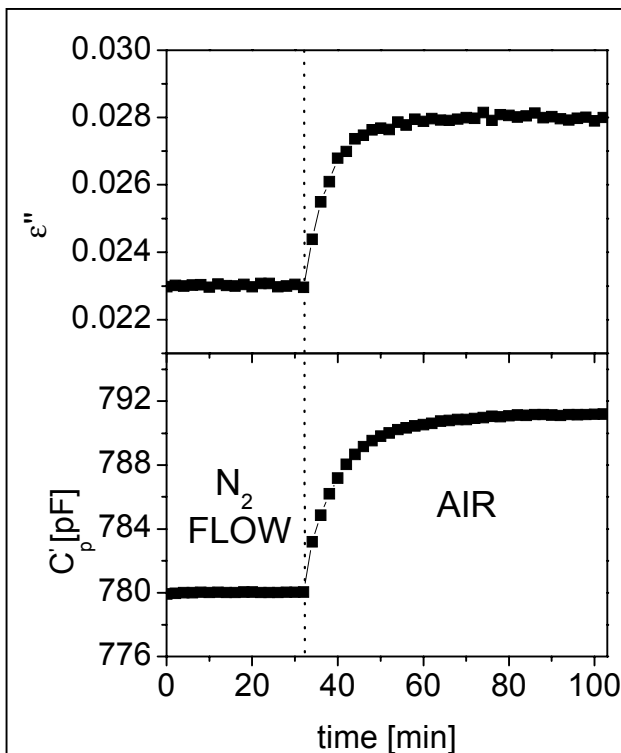


Fig. 1. Time dependence of the dielectric loss and sample capacitance at 24 °C and 0.1 MHz for a thin PS film of 20 nm in a pure nitrogen atmosphere and in ambient air.

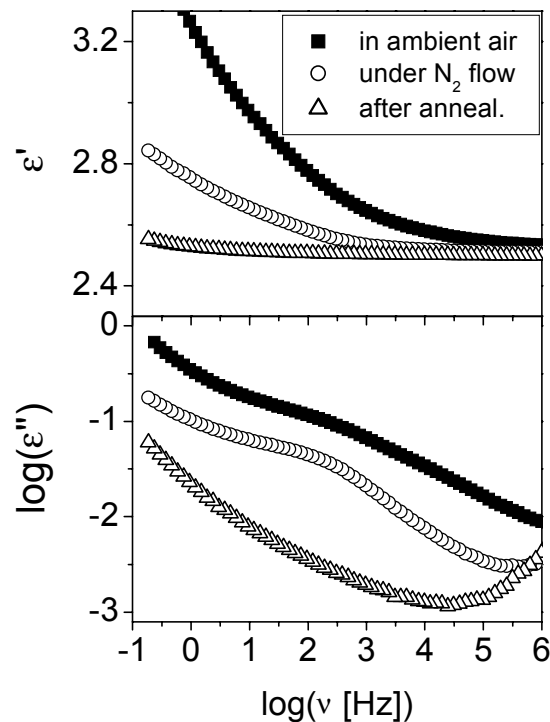


Fig. 2. ϵ' and ϵ'' vs. frequency at 25 °C for a thin PS film of 223 nm, in ambient air, under pure nitrogen flow and after annealing 2 hours at 135 °C.

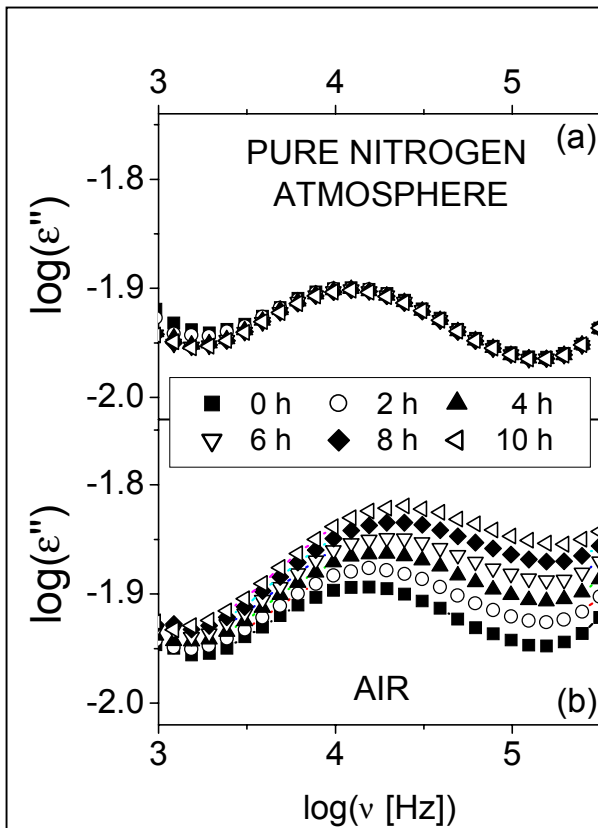


Fig. 4. Dielectric loss vs. frequency at 414 K showing the dynamic glass transition for a thin PS film of 84 nm in a pure nitrogen atmosphere (a) and in air (b).

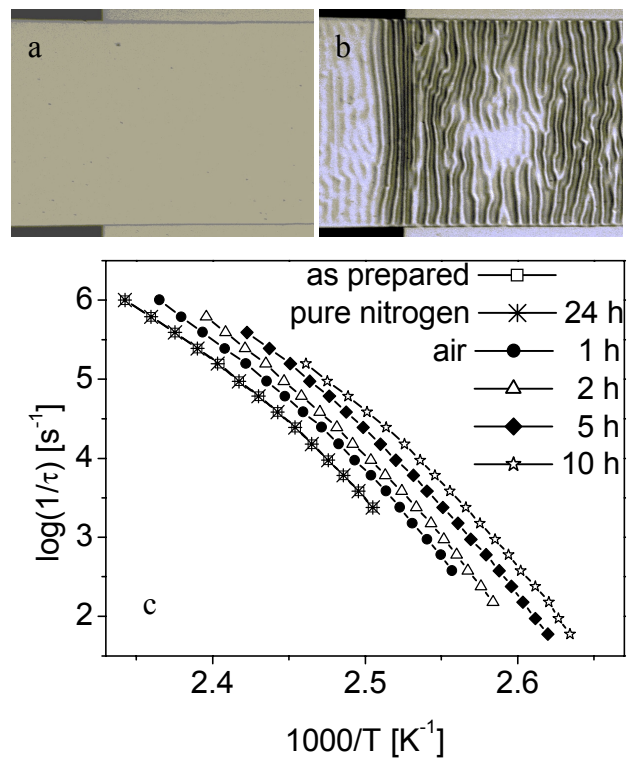


Fig. 5. a) optical image (top view) of the sample geometry for a thin PS film of 239 nm after 4 hours at 180 °C in a pure nitrogen atmosphere (~ 1 mm x 1 mm); b) the same sample after 4 hours at 180 °C in air (~ 1 mm x 1 mm); c) the relaxation rate of the dynamic glass transition vs. inverse temperature for a thin PS film of 63 nm after different annealing times at 180 °C in a pure nitrogen atmosphere and in air.

All measurements are performed with a Novocontrol Alpha analyzer and Quatro Cryosystem.

Despite the fact that polystyrene is hydrophobic in the bulk [17], pronounced water adsorption-desorption effects are detected in thin films (fig. 1, 2). This is a consequence of an enhanced surface-to-volume ratio, which increases by many orders of magnitude the area of exposure to ambient water-vapour. An example is given in fig. 1, for a thin PS film of 20 nm. When replaced from a dry nitrogen atmosphere and exposed to ambient air, the samples exhibit an increase in both their dielectric loss and the real part of the complex capacitance. Conversely, water-desorption effects are detected as well. The real part of the dielectric function ϵ' and the dielectric loss ϵ'' show a pronounced decrease when thin PS films are measured in a pure nitrogen atmosphere and after 2 hours of annealing at 135 °C (fig. 2).

Similar effects are observed even at temperature well-above the glass transition (fig. 3). When a thin PS film of 63 nm is kept at 180 °C in vacuum (~ 4 mbar), the real part of

the complex capacitance, a parameter sensitive to changes in the sample geometry and ϵ' , remains constant, proving sample stability under these conditions. To investigate the effects of water adsorption, Millipore water is injecting in the vacuum chamber through a vacuum-tight membrane. In the presence of water vapour, at the same annealing temperature, a sudden increase of the real part of the complex capacitance is observed, due to water adsorption. After this, the capacitance starts to increase continuously in time, accompanying a gradual change of the sample geometry. Hence, it is indicated that thin polymer films exhibit an enhanced mobility in the presence of water-vapour.

This can be directly proven by measuring the molecular dynamics of thin PS films under different experimental conditions using Broadband Dielectric Spectroscopy. While in a pure nitrogen atmosphere, no changes are detected during annealing at 414 K (fig. 4a), the dynamic glass transition becomes faster in time when the same thermal treatment is performed in ambient air

(fig. 4b). Even more pronounced effects are observed at higher temperatures (fig. 5). Annealing in ambient air at 180 °C leads to an increasingly faster dynamics, accompanied by a gradual change of the sample geometry which ends up with the formation of characteristic undulated pattern [18] (fig. 5b). After a similar annealing procedure in a pure nitrogen atmosphere, *no* changes in both the sample geometry and the relaxation rate of the dynamic glass transition are detected.

Measurements by IR-spectroscopy have revealed the formation of carbonyl C=O groups during the annealing in ambient air [18], which indicates that the origin of the enhanced mobility must be related to the oxidation of thin PS films. This causes chain scissions, which result in a decrease of the average molecular weight and, consequently, in a reduction of the glass transition temperature.

In conclusion, thin polymer films exhibit pronounced changes of their molecular dynamics when exposed to water-vapour and oxygen. To avoid possible plasticizer and chain-

scission effects, and by that, to deliver reliable experimental results, the measurements have to be performed in an inert atmosphere, i.e. in pure nitrogen or in high vacuum.

References

[1] L. Petychakis, G. Floudas, G. Fleischer, *Europhys. Lett.* **40**, 685 (1997).
 [2] A. Schönhalz et al., *Eur. Phys. J. E* **12**, 173-178 (2003).
 [3] A. Huwe, F. Kremer, P. Behrens, and W. Schwieger, *Phys. Rev. Lett.* **82**, 2338 (1999).
 [4] M. Arndt, et al., *Phys. Rev. Lett.* **79**, 2077 (1997).
 [5] Y. Grohens et al., *Langmuir* **14**, 2929 (1998).
 [6] J. L. Keddie, R. A. L. Jones, and R. A. Corry, *Europhys. Lett.* **27**, 59 (1994).
 [7] M. Wübbenhorst, C. A. Murray, J. R. Dutcher, *Eur. Phys. J. E direct* **12**, S109-S112, (2003).
 [8] J.A. Forrest, K. Dalnoki-Veress, J. R. Stevens J. R. Dutcher, *Phys. Rev. Lett.* **77**, 2002 (1996).
 [9] J.S. Sharp, J.A. Forrest, *Phys. Rev. E* **67**, 031805 (2003).
 [10] A. Serghei, F. Kremer, *Phys. Rev. Lett.* **91**, 165702 (2003).
 [11] K. Fukao, Y. Miyamoto, *Phys. Rev. E* **64**, 011803 (2001).
 [12] J. A Forrest, *Eur. Phys. J. E* **8**, 261 (2002).
 [13] L. Hartmann, F. Kremer, P. Pouret, L. Léger, *J. Chem. Phys.* **118**, 6052 (2003).
 [14] M. Yu. Efremov et al., *Phys. Rev. Lett.* **91**, 085703 (2003).
 [15] V. Lupascu et al., *Thermochimica Acta* **432**, 222 (2005).
 [16] A. Serghei, F. Kremer, *Progress Colloid Polym. Sci.*, in press (2005).
 [17] *Polymer Handbook*, fourth edition, edited by J. Brandrup, E.H. Immergut, E.A. Gulke, John Wiley & Sons, Inc., USA (1999).
 [18] A. Serghei, et al. *Phys. Rev. E* **71**, 061801 (2005).

A. Serghei, Prof. F. Kremer
 University of Leipzig, Department of Physics, Linnéstrasse 5,
 04103 Leipzig, Germany

G. Schaumburg

New Turnkey Solution for Dielectric and Impedance Spectroscopy up to 1400 °C

One of Novocontrol's strengths is to supply turnkey systems for dielectric, impedance and electrochemical impedance spectroscopy including sample cells and temperature control systems.

For applications requiring higher temperatures, Novocontrol introduces the new Concept 44 series. These systems operate from ambient up to a maximal temperature of 1200 or 1400 °C. A photograph is shown in fig. 1. The systems are turn key mounted in a half size 19" rack containing a high temperature furnace, temperature controller, furnace power supply and a high temperature sample cell mounted on an adjustable holder.

hermetically sealed sample cell

The sample cell consists of
 -a base unit with BNC connectors

for up to four sample electrodes, three temperature sensors and two channels for gas supply or cell evacuation,

- an inner ceramic tube which holds the sample at its upper end,
- an outer ceramic tube which surrounds the cell.

For sample preparation, the cell is moved out of the furnace by the cell holder. After removing the outer ceramic tube from the cell, the sample is prepared as shown in fig. 2. The sample is typically

- a flat disk with about 20 mm diameter with evaporated metal electrodes at both sides

or

- a cylinder with about 20 mm length with metal electrodes applied at each cylinder end and one or two optional ring electrodes in-between.

2, 3 or 4 wire or electrode configurations

The sample can be connected to the impedance analyzer by 2, 3 or 4 wires. The 2 wire set-up as shown in fig. 2 is simplest, easiest to prepare and provides best isolation properties. It is therefore recommended for

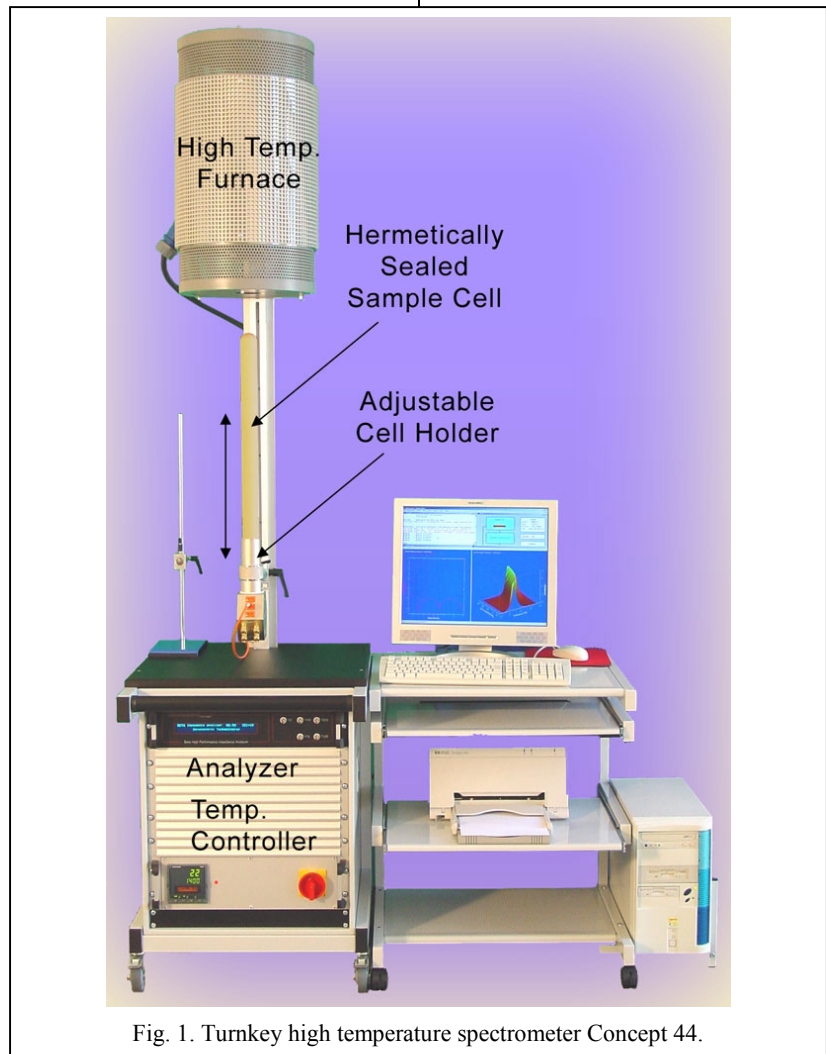


Fig. 1. Turnkey high temperature spectrometer Concept 44.

high insulating dielectric samples for which wire and electrode effects can be neglected.

4 wire configurations may be used in order to cancel out the wire impedance. In this case two pairs of voltage and current wires are connected to each other close to the sample and are further connected to 2 sample electrodes as shown in fig. 3a. This configuration does not cancel out electrode effects like contact impedance or electrode polarization. These effects can be reduced by a 4 electrode set-up as shown in fig. 3b. On the other hand, in this configuration the impedance Z_{in} of the two additional voltage electrodes to system ground may affect the measurements. Therefore, this configuration can be advantageously used if Z_{in} is high compared to both the sample and voltage electrode contact impedance.

especially advantageous with ZG4 and POT/GAL test interfaces

Z_{in} consists of the wire and BNC cable capacity (about 100 pF/m BNC cable length) to system ground and the impedance analyzer voltage channel input impedance which is typically $30 \text{ pF} \parallel 10^6 \Omega$ for standard analyzers. Z_{in} can be significantly reduced if a ZG4 or POT/GAL interface of the Novocontrol modular Alpha-A analyzer series [1] is used. These interfaces have a much higher input impedance of $10 \text{ pF} \parallel 10^{12} \Omega$ and can reduce the cable capacity by driven shield techniques. In addition, the cable length can be kept short by locating the interface close to the sample.

controlled gas flows or vacuum

Especially at higher temperatures, the sample properties may change in dependence of the surrounding atmosphere. Therefore the sample cell has separate gas flow channels both for the inner and outer ceramic

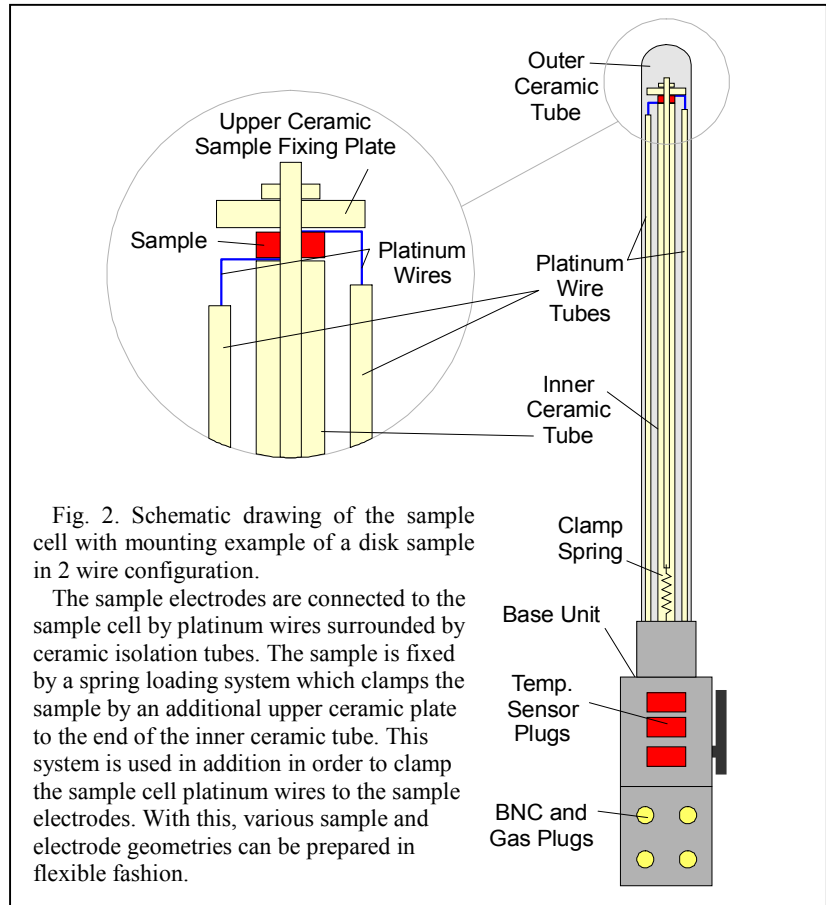


Fig. 2. Schematic drawing of the sample cell with mounting example of a disk sample in 2 wire configuration.

The sample electrodes are connected to the sample cell by platinum wires surrounded by ceramic isolation tubes. The sample is fixed by a spring loading system which clamps the sample by an additional upper ceramic plate to the end of the inner ceramic tube. This system is used in addition in order to clamp the sample cell platinum wires to the sample electrodes. With this, various sample and electrode geometries can be prepared in flexible fashion.

tubes. This allows to apply different gasses on each sample side and measure the impedance spectrum in dependence of gas type and concentration. As an alternative, the entire cell can be evacuated.

shielding by metal tube

The outer ceramic tube is shielded by an additional high temperature metal alloy tube against electrical stray fields from the furnace. This allows measurements of high insulating samples up to the T Ω range without electrical interference from the surrounding.

optional gas dosing and mixing

A gas control system for various

gasses can be supplied as an option. It consists of mass flow controllers with computer interface so that it is convenient to control gas dosing and mixing by the software that has been developed for this application.

The gas supply system provides a variety of possibilities as for instance obtaining gradients in activities of samples in nitrogen, oxygen, carbon, methane, etc.

Nitrogen may be used for purging and as an economical substitute for argon.

typical applications

This turnkey system allows dielectric and impedance measurements at high temperatures and controlled atmosphere on samples like electroceramics, semiconductors, ferroelectrics, solid-oxide-fuel-cell (SOFC) membranes, gas sensors, etc. Various shapes of platinum contacts to measure surface or bulk properties are supplied with the system.

References

[1] G. Schaumburg, Second Generation Alpha-A Dielectric, Conductivity, Impedance and Gain Phase Modular Measuring System, DNL July 2004

Dr. G. Schaumburg
Novocontrol Technologies, Germany

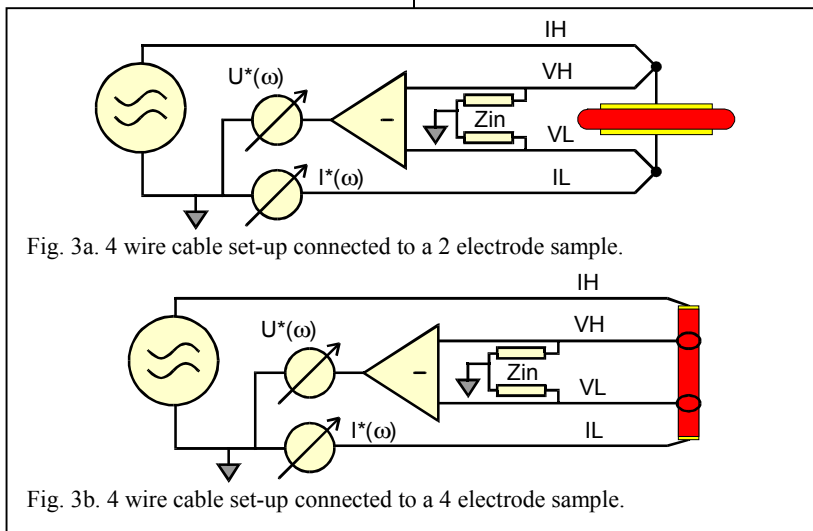
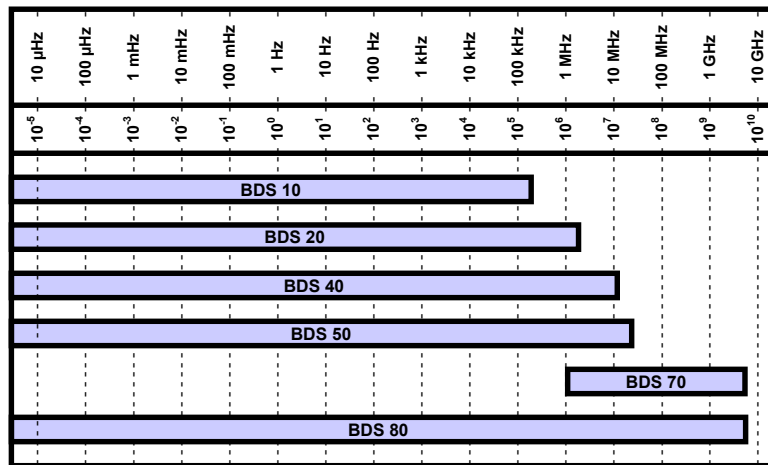


Fig. 3a. 4 wire cable set-up connected to a 2 electrode sample.

Fig. 3b. 4 wire cable set-up connected to a 4 electrode sample.

OVERVIEW

BROADBAND DIELECTRIC AND IMPEDANCE SPECTROSCOPY over 16 decades by Novocontrol Technologies



Factory and Head Office

NOVOCONTROL TECHNOLOGIES GmbH & Co. KG

Germany

Obererbacher Straße 9
D-56414 Hundsangen / GERMANY
Phone: ++49 64 35 - 96 23-0
Fax: ++49 64 35 - 96 23-33
Mail: novo@novocontrol.de
Web: www.novocontrol.de

Contact: Mr. den Dulk

United Kingdom

Additional Technical and Sales Support for British Customers
Headways, Shoulton, Hallow,
Worcester WR2 6PX / United Kingdom
Phone: ++(0) 870 085 0744
Fax: ++(0) 870 085 0745
Mail: jed@novocontrol.de

Contact: Mr. Jed Marson ++(0) 7974 926 166

Agents:

USA/Canada

NOVOCONTROL America, Inc.
8537 Purnell Ridge Road
Wake Forest, NC 27587
USA
Phone: +1 919 554 9904 Toll free: +1-866 554 9904
Fax: +1 919 556 9992
Mail: novocontrolusa@earthlink.net
Contact: Mr. Joachim Vinson, PhD

Japan

Morimura Bros. Inc.
2 nd chemical division
Morimura Bldg. 3-1, Toranomon 1-chome
Minato-Ku, Tokyo 105 / Japan
Phone ++(0) 3-3502-6440
Fax: ++(0) 3-3502-6437
Mail: hasegawa@morimura.co.jp
Contact: Mr. Hasegawa

Greece

Theodorou Automation SA
113 Geraka str
PO Box 67 868
15344 Gerakas / Greece
Tel: ++30 1 6047000
Fax: ++30 1 6046230
Mail: test@theodorou.gr
Contact: Mr. George Koukas

People's Rep. Of China

GermanTech Co. Ltd
Room 706, No. 7 Building, Hua Qing Jia Yuan
Wu Dao Kou, Haidian District
Beijing, 100083 / China
Mobile ++ 13501128834
Phone ++(10) 82867920/21/22
Fax: ++(10) 82867919
Mail: contact@germantech.com.cn

Benelux countries

NOVOCONTROL Benelux B.V.
Postbus 231
NL-5500 AE Veldhoven / NETHERLANDS
Phone ++(0) 40-2894407
Fax ++(0) 40-2859209

South Korea

WonATech
8-6 Woomyun-Dong, Seocho-Gu
Seoul 137-900, Korea
Phone ++ 82-2-578-6516
Fax: ++ 82 2-576-2635
Mail: jhkim@electrochemistry.co.kr
Contact: Mr. Jong Hyun Kim

Taiwan

JIEHAN Technology Corporation
No. 58, Chung Tai East Road, 404
Taichung / Taiwan
Phone ++886-4-2208-2450
Fax: ++886-4-2208-0010
Mail: jiehantw@ms76.hinet.net
Contact: Mr. Peter Chen

Middle East

National Scientific Company Ltd.
P.O.Box 437
Riyadh 11411 K.S.A.
Phone +966 1 473 6284
Fax +966 1 473 7759
Mail: nsc@diginet.sa
Contact: Mr. Osama Ali

Editor Dielectrics Newsletter: Gerhard Schaumburg. Abstracts and papers are always welcome. Please send your script to the editor